Animal Diseases

ORIGINAL ARTICLE

Open Access

Involvement of 2′-5′ oligoadenylate synthetase-like protein in the survival of *Mycobacterium tuberculosis* avirulent strain in macrophages

Aikebaier Reheman[1,2†], Xiaojian Cao[1,3†], Yifan Wang[1], Xi Nie[1], Gang Cao[1,3], Wei Zhou[1], Bing Yang[1], Yingying Lei[1], Weipan Zhang[1], Muhammad Ahsan Naeem[1,4] and Xi Chen[1*]

Abstract

Mycobacterium tuberculosis (*M. tuberculosis*) can replicate in the macrophage by interfering with many host protein functions. While it is far from known these host proteins for controlling *M. tuberculosis* infection. Herein, we infected macrophages including THP-1 and Raw264.7 cells with *M. tuberculosis* and identified the differentially expressed genes (DEGs) in the interferon signaling pathway. Among them, 2′-5′ oligoadenylate synthetase-like (OASL) underwent the greatest upregulation in *M. tuberculosis*-infected macrophages. Knockdown of the expression of OASL attenuated *M. tuberculosis* survival in macrophages. Further, bioinformatics analysis revealed the potential interaction axis of OASL-TAB3- Rv0127, which was further validated by the yeast-two-hybrid (Y2H) assay and Co-IP. This interaction axis might regulate the *M. tuberculosis* survival and proliferation in macrophages. The study reveals a possible role of OASL during *M. tuberculosis* infection as a target to control its propagation.

Keywords *Mycobacterium tuberculosis*, Interferon, Interferon stimulated genes, OASL

Introduction

Tuberculosis (TB), caused by *Mycobacterium tuberculosis* (*M. tuberculosis*), has been a leading bacterial infectious disease with high morbidity and mortality. In 2020, TB caused 1.2 million deaths (WHO 2020) and can maintain long-term survival in the host due to its escaping ability initiated by the host immune responses (Chen et al. 2021). The Interaction between *M. tuberculosis* and the host immune system remains elusive, pointing to the importance of this pathogen-host interaction for TB control.

Studies have reported that many cells are involved in the immune defense against *M. tuberculosis*, such as macrophages, dendritic cells, neutrophils, NK cells and some atypical T cells. (Liu et al. 2017). Thus, host innate immunity plays an important role in *M. tuberculosis* infection (Goldberg et al. 2014). As an important part of the host immune system, macrophages are the first line of defense against *M. tuberculosis* infection (Zhang et al. 2019). However, *M. tuberculosis* can evade the immune clearance of the macrophages through various host-pathogen

†Aikebaier Reheman and Xiaojian Cao have contributed equally to this work and share the first authorship.

*Correspondence:
Xi Chen
chenxi419@mail.hzau.edu.cn
[1] State Key Laboratory of Agricultural Microbiology, College of Veterinary Medicine, Huazhong Agricultural University, Wuhan 430070, China
[2] College of Animal Science and Technology, Tarim University, Alar 843300, China
[3] Bio-Medical Center, Huazhong Agricultural University, Wuhan 430070, China
[4] Department of Basic Sciences (Pharmacology), University of Veterinary and Animal Sciences (Narowal Campus), Lahore 54000, Pakistan

interaction pathways (Hmama et al. 2015). *M. tuberculosis* infection can alter gene expression profiles of host cells, and comparative analysis of gene expression profiles in different cells can facilitate a better understanding of the immunomodulatory effects of *M. tuberculosis* in macrophages.

Interferons play different roles during the invasion of *M. tuberculosis*. For example, the Type I IFN pathway plays a deleterious role for the host in mycobacterial infection by enhancing pathogen survival (Lai et al. 2020). However, type II interferons overcome *M. tuberculosis*-induced arrest of phagosome maturation, ensuring delivery of the bacterium to the phagolysosome, and leading to its elimination (Philips and Ernst 2012). IFN also acts as a host restriction factor to stimulate various host gene expression functions. As one of the IFN-stimulated genes (ISGs) family, 2′-5′ oligoadenylate synthetases-like (OASL) protein was more highly expressed in active TB patients' sera than that in latent TB patients' sera. However, it significantly decreased 6 months after treatment, indicating changes in the type I IFN response upon therapy (Sambarey et al. 2017). During *M. tuberculosis* infection, OASL is highly induced in host cells (Etna et al. 2015; Leisching et al. 2017a; Zhang et al. 2019) whereas, its biological role during infection is not completely clear.

In the current study, we analyzed the gene expression profiles in the two types of macrophages after *M. tuberculosis* infection and found the interferon signaling pathway genes as highly enriched among differentially expressed genes (DEGs) of macrophages. Among them, the expression of OASL was significantly up-regulated in macrophages infected with *M. tuberculosis*, and the intracellular survival ability of *M. tuberculosis* was attenuated after its knockdown. Further research shows that OASL may affect the intracellular survival of *M. tuberculosis* through the OASL-TAB3-Rv0127 interaction axis. Collectively, the IFN signaling pathway plays a significant role during the *M. tuberculosis* infection, and the OASL is likely to become the potential target for developing new TB treatments.

Results

M. tuberculosis induces differential expression of interferon and its stimulated genes in macrophages

Macrophages are the main targeted cells during *M. tuberculosis* infection. To further investigate the potential restriction factor of host immune cells for controlling bacterial survival, THP1, and Raw 264.7 cells were infected with *M. tuberculosis* for RNA-seq (Fig. 1A). The Reactome enrichment was performed for the differentially expressed genes (DEGs) between *M. tuberculosis*-infected cells and the control groups to annotate their related pathways. Our results showed that the up-regulated DEGs were enriched in IFN signaling-related pathways (Fig. 1B and C).

The cnet plot was then generated and found that most of the up-regulated ISGs were enriched in interferon signaling-related pathways (Fig. 1D). Among these genes, it was observed that IFNB1, ISG15, IFNL1, OAS1, OAS2, OAS3, and OASL were highly induced in THP-1 cells after *M. tuberculosis* infection (Fig. 1E). Whereas, ISG15, MAP2K6, OAS1A, OAS2, OASL1, and OASL2 were highly induced upon *M. tuberculosis* infection for 3 days in Raw264.7 cells (Fig. 1F). The qRT-PCR results showed that OASL and its homologous gene OASL2 expression were significantly higher than that of other genes in THP-1 cells and Raw264.7 (Fig. 1G and H). The results suggest that OASL and homologous genes may play key regulatory roles during *M. tuberculosis* infection of macrophages.

OASL facilitates *M. tuberculosis* survival in macrophages

It has been reported that OASL plays a critical role in defining the outcome of pathogen infection (Leisching et al. 2017b). The expression of OASL was validated by western blot and we found that the expression of OASL was significantly increased at day 3 post-infection in THP-1 cells compared to uninfected cells (Fig. 2A). To figure out the role of OASL in *M. tuberculosis* survival in macrophages, we designed three gRNAs to interfere with the expression of OASL which became significantly decreased in THP-1 cells carrying gRNAs targeting OASL compared to gRNA control (Fig. 2B, C). To investigate whether interfering OASL expression affects *M. tuberculosis* survival in macrophages, intracellular bacteria counting was performed. We found that the number of *M. tuberculosis* per cell was significantly decreased at day 3 post-infection (Fig. 2D, E). Furthermore, the viable intracellular bacteria assay showed a significantly decreased number of viable *M. tuberculosis* in OASL knocked down THP-1 cells compared to the gRNA control at day 3 post-infection (Fig. 2F). Hence, our result indicated that the high expression of OASL can promote *M. tuberculosis* survival in THP-1 cells.

Expression profile of OASL and its interaction genes

To identify other host proteins that participate in OASL-mediated intracellular survival of *M. tuberculosis*, the potentially interacted proteins with OASL were analyzed using STRING. The results showed that RSAD2, MX1, MX2, IFI6, ISG15, IRF7, IFIT1, IFIT2, IFIT3, and IFI35 might interact with human OASL (Fig. 3A), and RNA seq data showed that all of them were highly expressed in *M. tuberculosis*-infected THP-1 cells (Fig. 3B). qRT-PCR results have also shown increased expression of ISG15, IFIT1, IFIT2, IFIT3,

(See figure on next page.)

Fig. 1 Differential expression of interferon and its stimulated genes in macrophages after *M. tuberculosis* infection; **A** Schematic of infection of *M. tuberculosis* in different macrophages; **B**–**C** Reactome pathway enrichment analysis of differential expression genes (DEGs) in the macrophages; **D** The cnet plot was generated for interferon and its stimulated genes; **E** Gene expression profile of IFNs and ISGs in the THP-1 cells by RNA-Seq; **F** Gene expression profile of IFNs and ISGs in the Raw264.7 cells by RNA-Seq; **G**–**H** RNA-Seq data were validated by qRT-PCR in human and murine macrophages respectively. Data presented by mean ± SEM. All experiments were performed in triplicate. The values of $*p < 0.05$ were considered a statistically significant difference

and MX1 in THP-1 cells after *M. tuberculosis* infection (Figs. 1G and 3C). For Raw 264.7 cells, MX1, MX2, IFIT1, IFIT2, IFIT3, IRF7, RSAD2, DDX58, OASL1, and USP18 were predicted to interact with OASL2 (Fig. 3D). These proteins were highly expressed in *M. tuberculosis*-infected Raw264.7 cells compared to the uninfected control (Fig. 3E). The expression of MX2, IFIT3, and USP18 in Raw 264.7 cells was confirmed by using qRT-PCR (Fig. 3F).

Further, we examined the expression of IFIT1, IFIT2, IFIT3, and MX1 in both OASL knockdown THP-1 cell lines and wild-type THP-1 cells with or without *M. tuberculosis* infection. The results showed that IFIT1, IFIT2, IFIT3, and MX1 expression significantly decreased in OASL knockdown THP-1 cells relative to wild-type THP-1 cells after *M. tuberculosis* infection (Fig. 3G-J), indicating that these genes might be involved in the OASL-mediated intracellular survival of *M. tuberculosis* in THP-1 cells.

OASL promotes intracellular survival of *M.tuberculosis* may be mediated by Rv0127

To investigate whether the high-level OASL expression promotes *M. tuberculosis* survival through interaction with *M. tuberculosis* proteins, a yeast-two-hybrid (Y2H)-based protein-protein interaction (PPI) network was applied to identify the OASL-interacting proteins in *M. tuberculosis*. The results showed that OASL2, the alias protein of OASL, was found to interact with transforming growth factor β-activated kinase binding protein 3 (TAB3), which interacts with Rv0127 of *M. tuberculosis* (Fig. 4A). Thus, we hypothesized that the OASL-TAB3-Rv0127 axis may facilitate the survival of *M. tuberculosis* in the host cells. To confirm this hypothesis, we performed a Y2H assay which showed TAB3 interaction with *M. tuberculosis* protein Rv0127 (Fig. 4B). To verify this interaction axis, we have conducted a Co-IP experiment and confirmed the interaction of OASL- TAB3 and TAB3-Rv0127 (Fig. 4C, D). In addition, the qRT-PCR results showed that the expression of TAB3 was significantly increased in THP-1 cells after infection with *M. tuberculosis* relative to the uninfected control, however, there is no significant difference between OASL knockdown THP-1 cells infected with *M. tuberculosis* and uninfected control (Fig. 4E). Therefore, there was a potential interaction between OASL-TAB3-Rv0127 (Fig. 4F).

Discussion

As an intracellular pathogen, *M. tuberculosis* can alter the immune response to prevent itself from being cleared by the host immune cells through interaction with host proteins. Thus, host-pathogen interaction determines the outcome following infection by *M. tuberculosis. M. tuberculosis* was engulfed by macrophages, epithelial and endothelial cells (Baltierra-Uribe et al. 2014; Chen et al. 2015; Fine et al. 2012), and has a distinct fate, among which THP-1 cells provided *M. tuberculosis* the best shelter. This suggested that different cells are equipped with different defense machinery to clear invaded bacteria (Chen et al. 2021). Herein, we found that the up-regulated genes of macrophages after *M. tuberculosis* infection are enriched in IFN signaling-related pathways. Earlier studies also reported that *M.tuberculosis* infection of macrophages changed the gene expression levels of macrophages, and most of the up-regulated genes were enriched in innate immune response pathways, inflammation-related pathways, and immune regulation pathways (Lee et al. 2019; Ragno et al. 2001; Roy et al. 2018; Ehrt et al. 2001). These results are consistent with our results that the up-regulated genes are enriched in immune-related signaling pathways, which play a key role in the host-pathogen interaction process. Considering the ability of *M. tuberculosis* to exhibit long-term persistence and proliferation within macrophages, we hypothesized that interferon signaling might regulate *M. tuberculosis* survival.

Some studies have featured *M. tuberculosis* to elicit type I IFNs (Collins et al. 2015; Wassermann et al. 2015), whereas, the IFN signaling pathway also influenced the host immune response during *M. tuberculosis* infection, particularly by type I and type II (IFNs) (Lai et al. 2020). We found that IFNs and ISGs were differentially expressed in the macrophages, such as IFNB1, IFNL1, ISG15, and OASL. Among the highest upregulation of OASL, its role during *M. tuberculosis* infection was further studied and found that the number of intracellular

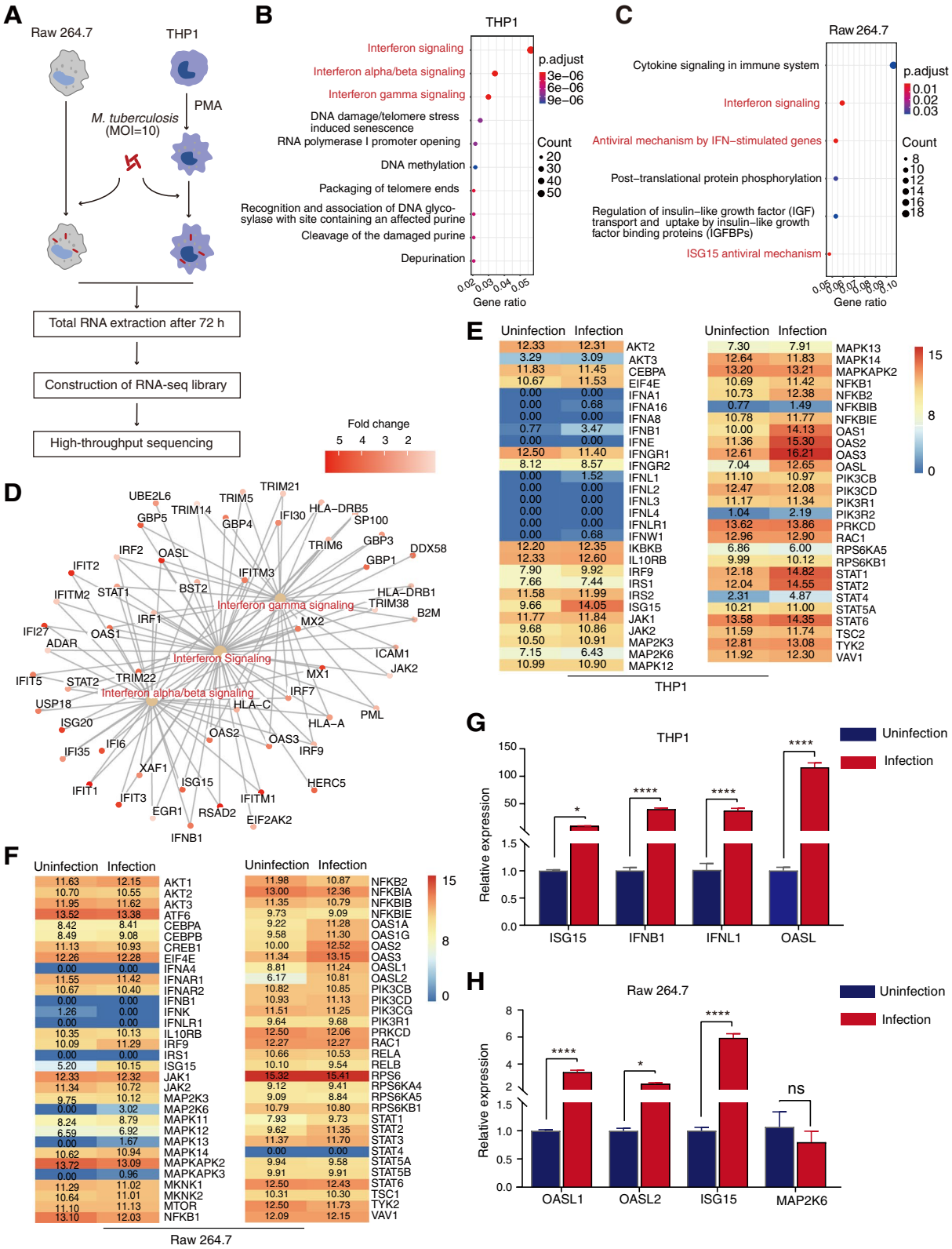

Fig. 1 (See legend on previous page.)

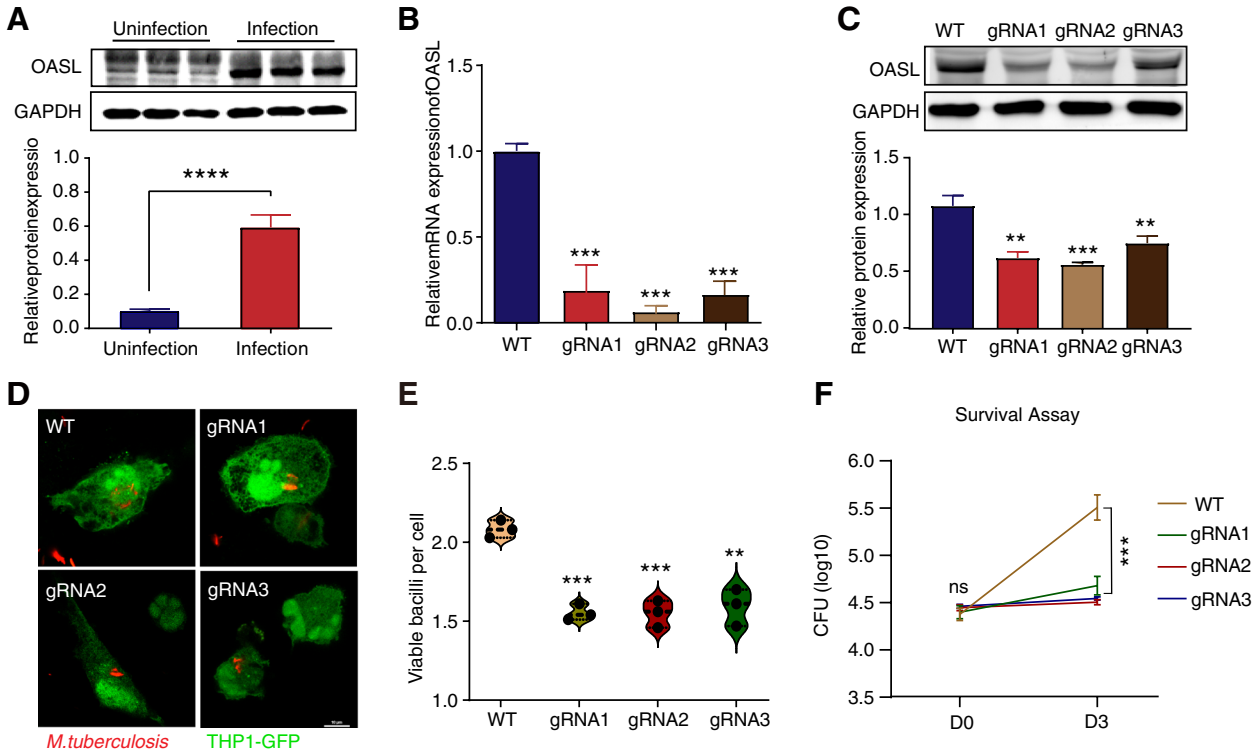

Fig. 2 OASL facilitates *M. tuberculosis* survival in the macrophages. **A** The protein expression level of OASL in THP-1 cells after *M. tuberculosis* infection, three repeats were shown for each sample; **B**–**C** The OASL knockdown efficiency in THP-1 cells was validated by qRT-PCR and western blot; **D** The visualization of *M. tuberculosis* in THP-1 cell lines using the confocal microscope, Scale bars = 10 μm; **E** The quantification of intracellular bacteria per cell; **F** Viable intracellular *M. tuberculosis* in THP-1 cell lines at day 0 and day 3 post-infection. Data presented by mean ± SEM. All experiments were performed in triplicate. The values of $*p < 0.05$ were considered a statistically significant difference

bacteria was significantly decreased in knocked-down OASL THP-1 cells, indicating that OASL facilitates *M. tuberculosis* survival in host cells. Therefore, we hypothesized that *M. tuberculosis*-induced OASL would have a critical role in the modulation of the anti-mycobacterial activity of host cells. However, the number of intracellular BCGs, hypovirulent, and hypervirulent *M. tuberculosis* increased when OASL was knocked down in macrophages (Leisching et al. 2020). The observed results contrast with those proposed in the current study, i.e. knock-down OASL inhibits *M. tuberculosis* replication. The possible reason could be that different strains, time points and MOI were used. Leisching et al. used hypovirulent R1507 at the MOI of 1 and analyzed the colony formation units (CFUs) at 24 and 96 h postinfection, while our study used *M.tuberculosis* H37Ra strain with MOI of 10, and the data were collected at 72 h postinfection. Therefore, we speculate that the differences in the experimental parameters may lead to different results.

The STRING analysis revealed that OASL interacts with IFIT1, IFIT2, IFIT3, MX1, and MX2, which are highly expressed in macrophages after *M. tuberculosis* infection, and the IFIT1, IFIT2, IFIT3, and MX1 expressions were reduced after OASL knockdown. The IFIT1, IFIT2, IFIT3, and MX1 genes are the important interferon-stimulating genes and are the most enriched type I interferon signaling pathways, which participate in various immune processes (Padariya et al. 2021).

The high expression of OASL could facilitate the survival of *M. tuberculosis* in the macrophages. However, the mechanism by which *M. tuberculosis* promotes the expression of OASL remains completely unclear. We speculated that OASL may interact with pathogenic proteins, thereby affecting the adaptation of pathogens to the host. Therefore, we analyzed the host-pathogen protein interaction network which was previously constructed by our team. Our PPI network results showed that OASL interacts with TAB3, which interacts with Rv0127 and this was confirmed by the Y2H assay and Co-IP experiment. Rv0127 encodes a maltose-1- phosphate synthetase (maltokinase, Mak), and it may be a potential drug target (Mendes et al. 2010). Genomic analysis studies have shown that the avirulent strain H37Ra genome is highly similar to the virulent strain H37Rv (Zheng et al. 2008), and the Ensembl Bacteria database has shown that Rv0127 exists in both virulent and avirulent strains

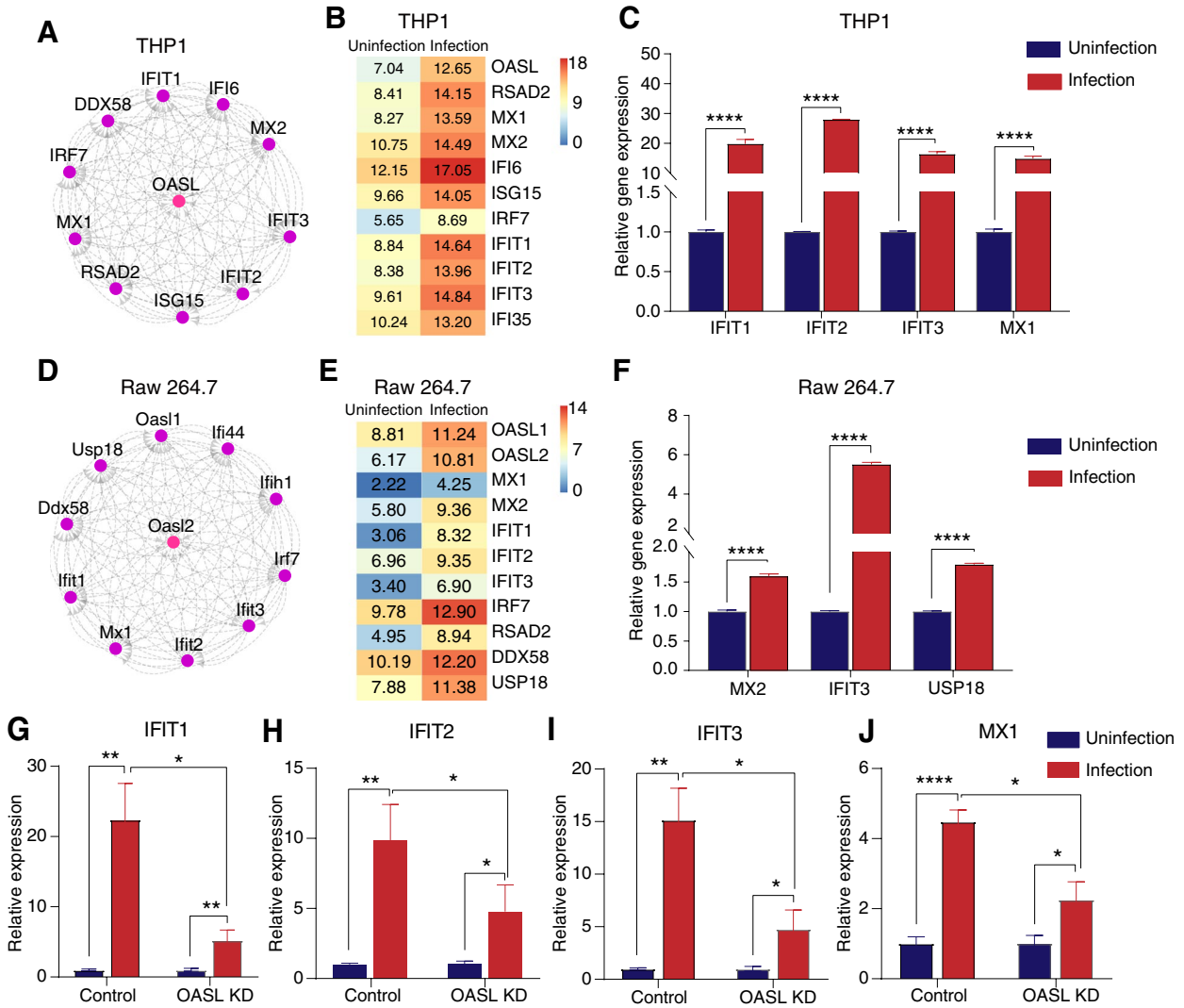

Fig. 3 OASL and its interacting proteins. **A** Interaction map prediction of human OASL with its interacting proteins by STRING; **B** Normalized count of OASL and its interaction protein-encoding genes in THP1 cells; **C** qRT-PCR validation of OASL interaction protein-encoding genes in THP1 cells; **D** Interaction map depicting prediction of murine OASL2 with its interacting proteins using STRING; **E** Normalized count of OASL2 and its interaction protein-encoding genes in Raw 264.7 cells; **F** qRT-PCR validation of OASL2 interaction protein-encoding genes in Raw 264.7 cells; **G**-**J** The expression of OASL interacting genes in the OASL knockdown THP-1 cell lines. Data presented by mean ± SEM. All experiments were performed in triplicate. The values of $*p < 0.05$ were considered a statistically significant difference

(http://bacteria.ensembl.org/true). Rv0127 was considered essential for virulent *M. tuberculosis* H37Rv growth (Mendes et al. 2010). TAB3 is a binding protein of TAK1 and *M. tuberculosis* effector protein PtpA partially inhibited the activation of the NF-κB pathway by selectively targeting TAB3 (Wang et al. 2015). Thus, our results suggested that OASL promotes the intracellular survival of *M. tuberculosis* during infection by modulating multiple host signaling pathways through the OASL-TAB3-Rv0127 axis.

Conclusions

This study demonstrates the critical role of OASL in restricting *M. tuberculosis* survival in macrophages. Therefore, OASL may be a potential target for the development of host-directed therapies.

Materials and methods

Bacteria and cells culture

M. tuberculosis strain H37Ra (ATCC 25177) was cultured in Middlebrook 7H9 broth (Becton Dickinson) supplemented with 0.5% glycerol, 0.05% Tween-80, and 10% oleic acid albumin dextrose catalase (OADC,

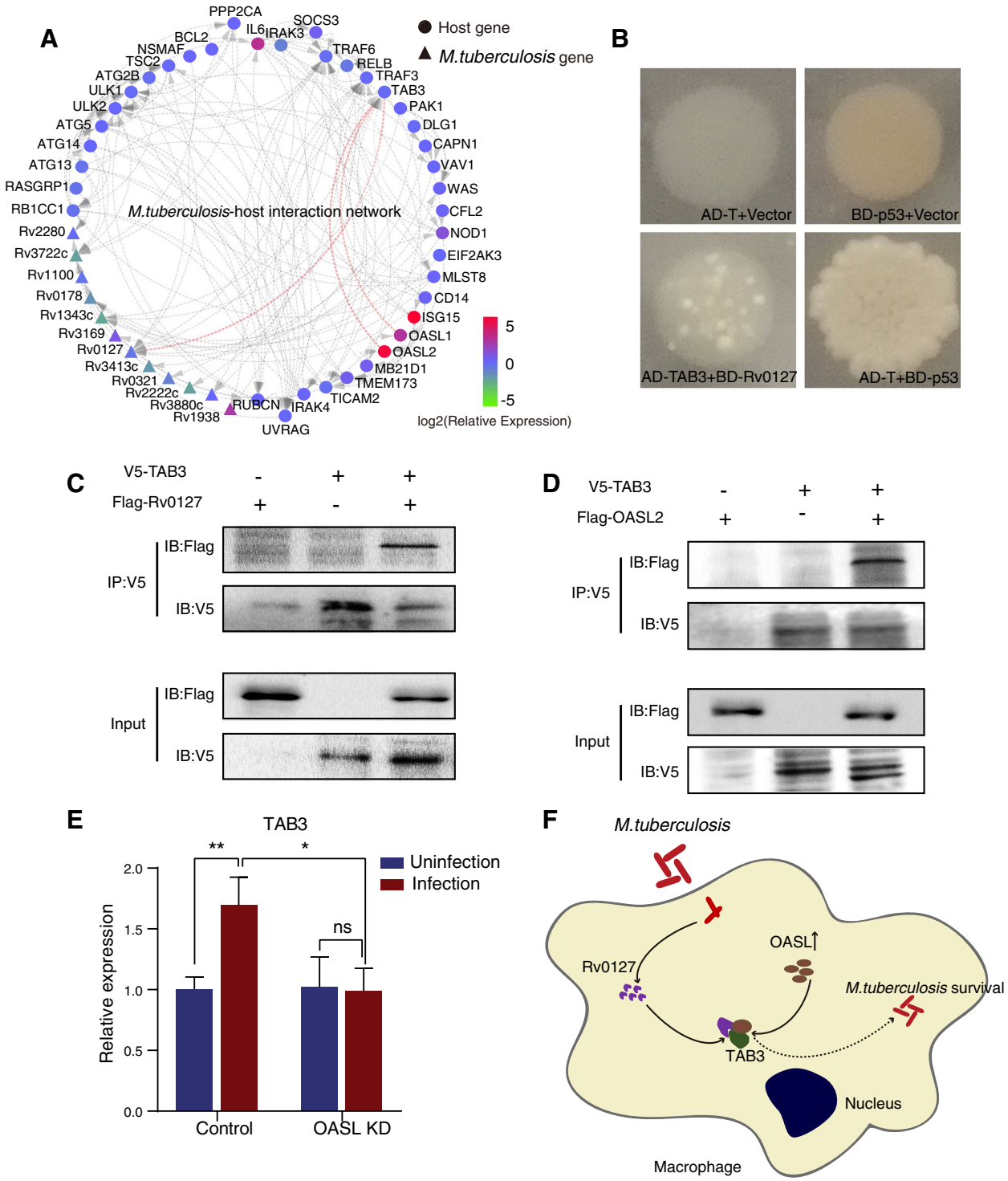

Fig. 4 The TAB3 mediates the indirect interaction between OASL and Rv0127. **A** The interaction network between *M. tuberculosis* protein and host proteins constructed by Y2H; **B** Validation of the interaction between TAB3 and Rv0127 by Y2H. Co-transformation of pmBD empty vector with pmAD vector containing T and co-transformation of the pmAD empty vector with pmBD vector containing p53 were used as negative controls. Co-transformation of pmAD vector containing T and pmBD vector containing p53 was used as positive controls. **C**–**D** Validation of protein-protein interactions by co-IP experiments. HEK 293T cells were co-transfected with V5-tagged TAB3 and Flag-tagged Rv0127, OASL2. Cells were harvested for Co-IP assays 36 h after transfection. Co-transfection of V5-tagged TAB3 with Flag-tagged empty vector and Flag-tagged Rv0127 with V5-tagged empty vector, Flag-tagged OASL2 with V5-tagged empty vector were used as negative controls; **E** The expression of TAB3 in different THP-1 cells before and after *M. tuberculosis* infection; **F** Schematic of how OASL may promote *M. tuberculosis* survival in macrophages. All experiments were performed in triplicate. The values of $*p < 0.05$ were considered a statistically significant difference

Becton Dickinson). For infection, the bacterial culture optical densities at 600 nm were adjusted to achieve the required MOI and centrifuged at 3000 g for 10 min to pellet the bacteria. The pellet was re-suspended in an infection medium and passed several times through an insulin syringe to disperse the bacteria. In addition, 50 µL from serially-diluted inoculation was plated to Middlebrook 7H11 agar (Becton Dickinson) to determine the number of viable bacteria (colony forming units - CFU).

The human monocytic cell line (THP-1, ATCC TIB-202) was maintained in RPMI-1640 medium supplemented with 10% FBS and was differentiated for 24 h using a culture medium containing 40 ng/mL phorbol 12-myristate 13-acetate (PMA) before infection. Murine macrophages (Raw 264.7, ATCC TIB-71TM) were maintained in Dulbecco's Modified Eagle's Medium (DMEM) supplemented with 10% fetal bovine serum (FBS).

RNA-Seq library preparation and sequencing

1×10^6 of cells were seeded into a 6-well plate and incubated with *M. tuberculosis* (MOI = 10) for 6 h. To stop infection, the cells were washed three times with pre-warmed PBS to remove extracellular *M. tuberculosis* and then supplied with a fresh medium with 5% FBS containing amikacin (50 mg/ml) (referred to as day 0). The cells were lysed with 1 mL of Trizol reagent at 72 h post-infection. Lysates were mixed with 0.2 mL of chloroform centrifuge for 10 min at 12,000 g at 4 °C. 0.4 mL of aqueous layer mixed with 0.4 mL of isopropanol in a new nuclease-free Eppendorf tube. The RNA was precipitated at room temperature for 10 min and pelleted by centrifuge for 10 min at 12,000 g. Eluted RNAs were washed twice with 75% ethanol. The quality and quantity of RNAs were examined by a Nanodrop 2000c spectrophotometer (Thermo Scientific).

The libraries were generated with VAHTS Stranded mRNA-seq Library Prep Kit (Vazyme Biotech Co., Ltd., China). Briefly, mRNAs were isolated using mRNA Capture Beads from 1 µg of total RNA and incubated for fragmentation at 94 °C for 8 min to get mRNAs with a length of 150 bp – 200 bp. The mRNAs were reverse-transcribed to cDNA and converted into double-stranded cDNA molecules. Following end-repairing and dA-tailing, the pair-ended sequencing adaptors were ligated to the ends of the cDNA fragments and then subjected to library amplification and purification. The purified libraries were validated and quantified using the Agilent 2100 Bioanalyzer (Agilent Technologies) and sequenced with the Hi-Seq X 10 instrument.

NGS data process and visualization

The RNA-seq data was processed into a reading count corresponding to each sample following Pertea et al.'s method (Pertea et al. 2016), then read count lists were merged into a matrix by an R package dpylr (https://CRAN.R-project.org/package=dplyr). The read count matrix was applied to DESeq2 (Love et al. 2014) for the differential analysis, the genes which abs(foldchange) > 2 and P value < 0.05 were considered as the significant up/down-regulation genes, meanwhile, the normalized count was also exported. The gene expression differential list corresponding to each sample was merged by cells using dpylr, and the merged gene list was Reactome enriched by R package clusterProfiler (Yu et al. 2012) and ReactomePA (Yu and He 2016), then visualized through R dotplot function. The cnet plot was generated by clusterProfiler. The pathway gene list was downloaded from pathcard (https://pathcards.genecards.org/), then the count matrix was enriched by the pathcard gene list through dpylr, and the enrichment was visualized by heatmap generated heatmap. The OASL interaction genes were drawn from STRING (https://string-db.org/), these genes were used for generated a gene list, then the normalized count matrix was enriched by this list and visualized by heatmap The PPI network between *M. tuberculosis* and the host was withdrawn from the previous study (Yang et al. 2018) and visualized by Cytoscape (Shannon et al. 2003).

Construction of OASL knockdown cell lines

Three gRNAs used for *oasl* gene knockdown were designed using E-CRISPR (http://www.e-crisp.org/E-CRISP/). Each gRNA was inserted into the pHKO-dCas9 plasmid to obtain pHKO-OASL-KD-gRNA1, pHKO-OASL-KD-gRNA2, pHKO-OASL-KD-gRNA3 or pHKO-gRNA control. Lentiviruses containing gRNA were packaged by transfecting pHKO-OASL-KD-gRNAs or pHKO-gRNA control with pSPAX, pMD.2G into 293 T cells. Lentiviruses were harvested after 48 h and were used to infect THP-1 cells. Subsequently, the section with puromycin (2 µg/ml) was carried out. The expression of OASL was examined through qRT-PCR. All gRNAs and primers are shown in Table 1.

qRT-PCR

The total RNAs were extracted from cells and animal tissues using RNAiso Plus reagent (Code No. 9109, TaKaRa, Japan) and then 500 ng of RNAs were reverse transcribed to cDNA using ReverTra Ace qPCR RT Master Mix with gDNA Remover Kit (Vazyme Biotech Co. Ltd., China) according to the manufacturer's instruction. SYBR Select Master Mix (TOYOBO, Japan) was used for PCR. PCRs were run on QuanStudio 6 real-time PCR system and relative expression was calculated using the $2^{-\Delta\Delta Ct}$ method. GAPDH was used as a control. Primers are shown in Table 1.

Table 1 Primers used in the study

Name	Forward Primer (5′-3′)	Reverse Primer (5′-3′)
OASL-sgRNA-1	CACCGGAGCATTTCCAGGGGAAGCG	AAACCGCTTCCCCTGGAAATGCTCC
OASL-sgRNA-2	CACCGGGTCCAGCCCACGCTTCCCC	AAACGGGGAAGCGTGGGCTGGACCC
OASL-sgRNA-3	CACCGGCGGGTGCTGAAGGTAGTCA	AAACTGACTACCTTCAGCACCCGCC
Human-ISG15	GTGGACAAATGCGACGAACC	TCGAAGGTCAGCCAGAACAG
Human-IFNB1	TCTCCTGTTGTGCTTCTCCAC	GCCTCCCATTCAATTGCCAC
Human-IFNL1	GGTGACTTTGGTGCTAGGCT	GGCCTTCTTGAAGCTCGCTA
Human-OASL	AACGTGGCAGAAGGGTACAG	TCAAGTGGATGTCTCGTGCC
Human-IFIT1	CTCTGCCTATCGCCTGGATG	AGCTTCAGGGCAAGGAGAAC
Human-IFIT2	AGCGAAGGTGTGCTTTGAG	GCTTGCCTCAGAGGGTCAAT
Human-IFIT3	GGGCAGACTCTCAGATGCTC	AACACACCTTCGCCCTTTCA
Human-MX1	GGCATAACCAGAGTGGCTGT	CATTACTGGGGACCACCACC
Human-TAB3	CAGTTGTACCACCCAAGCCA	TGGGTGTCATGGATGTCTGC
Human-GAPDH	GGTATCGTGGAAGGACTCATGAC	ATGCCAGTGAGCTTCCCGTTCAG
Mouse OASL1	CCAACAATGTGGCAGAAGGC	CACGGTCACCTGGATATCGG
Mouse OASL2	CCAACAATGTGGCAGAAGGC	CCAACCGGAGGAGGTTCTTC
Mouse-ISG15	TGGTACAGAACTGCAGCGAG	AGCCAGAACTGGTCTTCGTG
Mouse-MAP2K6	CCGCCTCGGGATTTAGACTC	TGACGCATCTTCTCCACCAC
Mouse-MX2	CCTATTCACCAGGCTCCGAA	CACAAACCCTGGCAATTCTCG
Mouse- IFIT3	CTTCAGAGGAGGCGAAGTCC	ACATCGGGGCTCTCCTTACT
Mouse-USP18	CCCTCATGGTCTGGTTGGTT	TCCTCTCTTCTGCACTCCGA
Mouse-GAPDH	AGGTCGGTGTGAACGGATTTGG	CGTTGAATTTGCCGTGAGTGGA

Western blot

5×10^6 THP-1 cells were seeded into a 6-well plate and differentiated with PMA for 24 h, the THP-1 cells were incubated with *M. tuberculosis* (MOI = 10) for 4 h. To stop infection, the cells were washed three times with pre-warmed PBS to remove extracellular *M. tuberculosis* and then supplied with a fresh medium with 5% FBS containing amikacin (50 mg/ml) (referred to as day 0). After 72 h, the cells were lysed with RIPA lysis buffer containing protease inhibitor with a cocktail and incubated for 10 min on ice. Total proteins were quantified using a bicinchoninic acid assay (Beyotime Biotechnology, China), and 50 μg total protein was loaded. Proteins were transferred to the PVDF membrane after separation by SDS-PAGE. The membrane was blocked with fat-free milk for 1 h at room temperature after washing three times with TBST. Rabbit anti-OASL polyclonal antibody in PBST (1:2000) was added and incubated overnight at 4 °C. The HRP conjugated anti-rabbit antibody (1:300) was applied to the membrane after washing three times, 5 min each time. The membrane was imaged using Bio-Rad ChemiDoc MP.

Intracellular bacterial viability assay

2.0×10^5 cells were seeded in a 24-well plate and differentiated with PMA for 24 h, and the THP-1 cells were incubated with *M. tuberculosis* (MOI = 10) for 4 h. To stop infection, the cells were washed three times with pre-warmed PBS to remove extracellular *M. tuberculosis* and then supplied with a fresh medium with 5% FBS containing amikacin (50 mg/ml) (referred to as day 0). The infected cells were lysed after 72 h infection using sterile 0.1% Tween-80 in water, and viable bacilli were enumerated by serial dilution of lysates and plating on Middlebrook 7H11 agar. CFUs were counted after 3 to 4 weeks of incubation at 37 °C an incubator. All the infections were performed in triplicate.

Confocal microscopy

For confocal microscopy, 2.0×10^5 cells (THP-1-GFP-sgRNA, THP-1-GFP-OASL-gRNA1, THP-1-GFP-OASL-gRNA2, and THP-1-GFP-OASL-gRNA3, respectively) per well were seeded onto coverslips in a 24-well plate and differentiated for 24 h with PMA. RFP-H37Ra (MOI = 10) was applied to the wells for 4 h infection at 37 °C in 5% CO_2. The cells were washed three times with pre-warmed PBS to remove extracellular *M. tuberculosis*, and supplied with a fresh medium with 5% FBS containing amikacin (50 μg/mL). The medium was changed every 2 days to avoid serum starvation-induced autophagy. The infected cells were fixed with 4% paraformaldehyde for 30 min on day 3 post-infection and the cells were washed three times with pre-warmed PBS. The specimens were

mounted onto microscope slides using a prolonged antifade reagent. Images were obtained with an Olympus confocal laser microscope system equipped with FV10 ASW Imaging Software (Version 4.2, Olympus). The number of bacteria from 150 cells was analyzed. All infections were performed in triplicate.

Yeast two-hybrid

The full length of Rv0127 and TAB3 were restriction cloned into pmBD and pmAD plasmids of the GAL4 Y2H system (Clontech, Mountain-view, CA, USA) respectively as described (Yang et al. 2018). pmAD-TAB3 was transformed into yeast strain Y187, and plated on SD/−T selective plates. pmBD-Rv0127 was transformed into yeast strain GoldY2H, and plated on SD/−L selective plates. GoldY2H cells harboring Rv0127 plasmid and Y187 cells harboring TAB3 plasmid were hybridized and selected on SD/Leu − Trp − His− Ade − selective plates. The yeast strains were transformed with the respective constructs and transformants were selected on minimal media lacking leucine and tryptophan (−LT). Interactions were assessed by growing trans-formants in liquid culture at 30 °C and spotting on SD/ Leu − Trp − His− Ade − selective plates. Plates were imaged after 3–5 d growth at 30 °C.

Co-IP assay

Immunoprecipitation and immunoblotting HEK293T cells were transiently transfected with pCDNA3.1-V5-TAB3 and pCAGGS-Flag-Rv0127, pCAGGS-Flag-OASL2. After 36 h, cells were washed with PBS, followed by western blotting and immunoprecipitation with cell lysis buffer (50 mM Tris-HCl, pH 7.5, 150 mM NaCl, 0.05% Nonidet P-40) with the addition of 1% protease inhibitors. Cocktail (Sigma, P8340). After 30 min incubation on ice, whole cell lysates were centrifuged at 10,000 g for 10 min at 4 °C to remove debris. Cell lysates were incubated with V5-tag mAb magnetic agarose beads (MBL, M180–10) overnight at 4 °C. Immune complex samples were centrifuged, washed 3 times with cell lysis buffer, and then boiled in SDS loading buffer for 5–10 min. After 12% separation by SDS-PAGE, equal amounts of protein were electro-blotted onto polyvinylidene fluoride membranes (Millipore, Bedford, MA, USA). Membranes were blocked with 0.05% Tween 20 (TBST) and 5% nonfat dry milk in triple buffered saline for 2 hr. at room temperature, followed by overnight incubation with primary antibodies (DDDDK-Tag Rabbit mAb, AE092, ABclonal; V5-Tag mAb, AE089, ABclonal). After washing 3 times with TBST, diluted with appropriate horseradish peroxidase-conjugated secondary antibody for 2 h at room temperature. Immuno-reactive protein bands were visualized by Western ECL clear substrate (BioRad, 1,705,060).

Statistical analysis

Numerical data were analyzed by GraphPad Prism 7.0 (La Jolla, CA) software from three independent experiments shown as mean ± SEM. Evaluation of the significance of differences between groups was performed by using one-way ANOVA or student t-test.

Acknowledgments

Confocal microscopy was conducted in and supported by the State Key Laboratory of Agricultural Microbiology at Huazhong Agricultural University.

Authors' contributions

Conceptualization, A.R. and X.J.C.; methodology, X.J.C., and Y.F.W.; software, X.J.C.; validation, A.R. and X.J.C.; formal analysis, X.N. and M.A.N.; investigation, G.C.; resources, X.C and G.C.; data curation, W.Z.; writing—original draft preparation, X.C.; writing—review and editing, A.R., X.C. and M.A.N.; visualization, A.R. and X.C.; supervision, B.Y., and Y.Y.L.; project administration, A.R. and W.P.Z.; funding acquisition, G.C and X.C.. All authors have read and agreed to the published version of the manuscript.

Funding

This research was funded by the National Natural Science Foundation of China (Grant No. 31602061, U21A20259, 31872470), and the National Key Research and Development Program of China (Grant No. 2021YFD1800401).

Availability of data and materials

The data sets used in this study are available in the following databases: Host RNA-Seq data: Gene Expression Omnibus GSE125907 and *M. tuberculosis* RNA-Seq data: Gene Expression Omnibus GSE162200.

Declarations

Ethics approval and consent to participate

This study does not involve animal ethics.

Consent for publication

Not applicable.

Competing interests

The authors declare no conflict of interest.

Received: 15 December 2022 Accepted: 16 February 2023
Published online: 02 March 2023

References

Baltierra-Uribe, S.L., M.D. Garcia-Vasquez, N.S. Castrejon-Jimenez, M.P. Estrella-Pinon, J. Luna-Herrera, and B.E. Garcia-Perez. 2014. Mycobacteria entry and trafficking into endothelial cells. *Canadian Journal of Microbiology* 60 (9): 569–577. https://doi.org/10.1139/cjm-2014-0087.

Chen, X., X. Cao, Y. Lei, A. Reheman, W. Zhou, B. Yang, W. Zhang, W. Xu, S. Dong, R. Tyagi, Z.F. Fu, and G. Cao. 2021. Distinct persistence fate of *Mycobacterium tuberculosis* in various types of cells. *mSystems* 6 (4): e0078321. https://doi.org/10.1128/mSystems.00783-21.

Chen, X., K. Sakamoto, F.D. Quinn, H.C. Chen, and Z.F. Fu. 2015. Lack of intracellular replication of M. tuberculosis and M. bovis BCG caused by delivering bacilli to lysosomes in murine brain microvascular endothelial cells. *Oncotarget* 6 (32): 32456–32467. https://doi.org/10.18632/oncotarget.5932.

Collins, A.C., H. Cai, T. Li, L.H. Franco, X.D. Li, V.R. Nair, C.R. Scharn, C.E. Stamm, B. Levine, Z.J. Chen, and M.U. Shiloh. 2015. Cyclic GMP-AMP synthase is an

innate immune DNA sensor for Mycobacterium tuberculosis. *Cell Host & Microbe* 17 (6): 820–828. https://doi.org/10.1016/j.chom.2015.05.005.
Ehrt, Sabine, D. Schnappinger, Stefan Bekiranov, Jörg Drenkow, Shuangping Shi, Thomas R. Gingeras, Terry Gaasterland, Gary Schoolnik, and Carl Nathan. 2001. Reprogramming of the macrophage transcriptome in response to interferon-gamma and Mycobacterium tuberculosis signaling roles of nitric oxide synthase2 and phagocyte oxidase. *The Journal of Experimental Medicine* 194: 1123–1139.
Etna, M.P., E. Giacomini, M. Pardini, M. Severa, D. Bottai, M. Cruciani, F. Rizzo, R. Calogero, R. Brosch, and E.M. Coccia. 2015. Impact of Mycobacterium tuberculosis RD1-locus on human primary dendritic cell immune functions. *Scientific Reports* 5: 17078. https://doi.org/10.1038/srep17078.
Fine, K.L., M.G. Metcalfe, E. White, M. Virji, R.K. Karls, and F.D. Quinn. 2012. Involvement of the autophagy pathway in trafficking of Mycobacterium tuberculosis bacilli through cultured human type II epithelial cells. *Cellular Microbiology* 14 (9): 1402–1414. https://doi.org/10.1111/j.1462-5822.2012.01804.x.
Goldberg, M.F., N.K. Saini, and S.A. Porcelli. 2014. Evasion of innate and adaptive immunity by Mycobacterium tuberculosis. *Microbiology Spectrum* 2 (5). https://doi.org/10.1128/microbiolspec.MGM2-0005-2013.
Hmama, Z., S. Pena-Diaz, S. Joseph, and Y. Av-Gay. 2015. Immunoevasion and immunosuppression of the macrophage by Mycobacterium tuberculosis. *Immunological Reviews* 264 (1): 220–232. https://doi.org/10.1111/imr.12268.
Lai, Y., G.H. Babunovic, L. Cui, P.C. Dedon, J.G. Doench, S.M. Fortune, and T.K. Lu. 2020. Illuminating host-mycobacterial interactions with genome-wide CRISPR knockout and CRISPRi screens. *Cell Systems* 11 (3): 239–251.e237. https://doi.org/10.1016/j.cels.2020.08.010.
Lee, J., S.G. Lee, K.K. Kim, Y.J. Lim, J.A. Choi, S.N. Cho, C. Park, and C.H. Song. 2019. Characterisation of genes differentially expressed in macrophages by virulent and attenuated Mycobacterium tuberculosis through RNA-Seq analysis. *Scientific Reports* 9 (1): 4027. https://doi.org/10.1038/s41598-019-40814-0.
Leisching, G., A. Ali, V. Cole, and B. Baker. 2020. 2′-5′-Oligoadenylate synthetase-like protein inhibits intracellular M. tuberculosis replication and promotes proinflammatory cytokine secretion. *Molecular Immunology* 118: 73–78. https://doi.org/10.1016/j.molimm.2019.12.004.
Leisching, G., R.D. Pietersen, C. van Heerden, P. van Helden, I. Wiid, and B. Baker. 2017a. RNAseq reveals hypervirulence-specific host responses to M. tuberculosis infection. *Virulence* 8 (6): 848–858. https://doi.org/10.1080/21505594.2016.1250994.
Leisching, G., I. Wiid, and B. Baker. 2017b. The association of OASL and type I interferons in the pathogenesis and survival of intracellular replicating bacterial species. *Frontiers in Cellular and Infection Microbiology* 7: 196. https://doi.org/10.3389/fcimb.2017.00196.
Liu, C.H., H. Liu, and B. Ge. 2017. Innate immunity in tuberculosis: Host defense vs pathogen evasion. *Cellular & Molecular Immunology* 14 (12): 963–975. https://doi.org/10.1038/cmi.2017.88.
Love, M.I., W. Huber, and S. Anders. 2014. Moderated estimation of fold change and dispersion for RNA-seq data with DESeq2. *Genome Biology* 15 (12): 550. https://doi.org/10.1186/s13059-014-0550-8.
Mendes, V., A. Maranha, P. Lamosa, M.S. da Costa, and N. Empadinhas. 2010. Biochemical characterization of the maltokinase from Mycobacterium bovis BCG. *BMC Biochemistry* 11: 21. https://doi.org/10.1186/1471-2091-11-21.
Padariya, M., A. Sznarkowska, S. Kote, M. Gomez-Herranz, S. Mikac, M. Pilch, J. Alfaro, R. Fahraeus, T. Hupp, and U. Kalathiya. 2021. Functional interfaces, biological pathways, and regulations of interferon-related DNA damage resistance signature (IRDS) genes. *Biomolecules* 11 (5): 622. https://doi.org/10.3390/biom11050622.
Pertea, M., D. Kim, G.M. Pertea, J.T. Leek, and S.L. Salzberg. 2016. Transcript-level expression analysis of RNA-seq experiments with HISAT, StringTie and Ballgown. *Nature Protocols* 11 (9): 1650–1667. https://doi.org/10.1038/nprot.2016.095.
Philips, J.A., and J.D. Ernst. 2012. Tuberculosis pathogenesis and immunity. *Annual Review of Pathology* 7: 353–384. https://doi.org/10.1146/annurev-pathol-011811-132458.
Ragno, S., M. Romano, S. Howell, D.J. Pappin, P.J. Jenner, and M.J. Colston. 2001. Changes in gene expression in macrophages infected with Mycobacterium tuberculosis: A combined transcriptomic and proteomic approach. *Immunology* 104 (1): 99–108. https://doi.org/10.1046/j.0019-2805.2001.01274.x.
Roy, S., S. Schmeier, B. Kaczkowski, E. Arner, T. Alam, M. Ozturk, O. Tamgue, S.P. Parihar, H. Kawaji, M. Itoh, T. Lassmann, P. Carninci, Y. Hayashizaki, A.R.R. Forrest, R. Guler, V.B. Bajic, F. Brombacher, and H. Suzuki. 2018. Transcriptional landscape of Mycobacterium tuberculosis infection in macrophages. *Scientific Reports* 8 (1): 6758. https://doi.org/10.1038/s41598-018-24509-6.
Sambarey, A., A. Devaprasad, A. Mohan, A. Ahmed, S. Nayak, S. Swaminathan, G. D'Souza, A. Jesuraj, C. Dhar, S. Babu, A. Vyakarnam, and N. Chandra. 2017. Unbiased identification of blood-based biomarkers for pulmonary tuberculosis by modeling and mining molecular interaction networks. *Ebiomedicine* 15: 112–126. https://doi.org/10.1016/j.ebiom.2016.12.009.
Shannon, P., A. Markiel, O. Ozier, N.S. Baliga, J.T. Wang, D. Ramage, N. Amin, B. Schwikowski, and T. Ideker. 2003. Cytoscape: A software environment for integrated models of biomolecular interaction networks. *Genome Research* 13 (11): 2498–2504. https://doi.org/10.1101/gr.1239303.
Wang, J., B.X. Li, P.P. Ge, J. Li, Q. Wang, G.F. Gao, X.B. Qiu, and C.H. Liu. 2015. Mycobacterium tuberculosis suppresses innate immunity by coopting the host ubiquitin system. *Nature Immunology* 16 (3): 237–U189. https://doi.org/10.1038/ni.3096.
Wassermann, R., M.F. Gulen, C. Sala, S.G. Perin, Y. Lou, J. Rybniker, J.L. Schmid-Burgk, T. Schmidt, V. Hornung, S.T. Cole, and A. Ablasser. 2015. Mycobacterium tuberculosis differentially activates cGAS- and inflammasome-dependent intracellular immune responses through ESX-1. *Cell Host & Microbe* 17 (6): 799–810. https://doi.org/10.1016/j.chom.2015.05.003.
WHO. 2020. Global tuberculosis report.
Yang, F., Y. Lei, M. Zhou, Q. Yao, Y. Han, X. Wu, W. Zhong, C. Zhu, W. Xu, R. Tao, X. Chen, D. Lin, K. Rahman, R. Tyagi, Z. Habib, S. Xiao, D. Wang, Y. Yu, H. Chen, Z. Fu, and G. Cao. 2018. Development and application of a recombination-based library versus library high- throughput yeast two-hybrid (RLL-Y2H) screening system. *Nucleic Acids Research* 46 (3): e17. https://doi.org/10.1093/nar/gkx1173.
Yu, G., and Q.Y. He. 2016. ReactomePA: An R/Bioconductor package for reactome pathway analysis and visualization. *Molecular BioSystems* 12 (2): 477–479. https://doi.org/10.1039/c5mb00663e.
Yu, G., L.G. Wang, Y. Han, and Q.Y. He. 2012. clusterProfiler: An R package for comparing biological themes among gene clusters. *OMICS* 16 (5): 284–287. https://doi.org/10.1089/omi.2011.0118.
Zhang, Y.W., Y. Lin, H.Y. Yu, R.N. Tian, and F. Li. 2019. Characteristic genes in THP-1 derived macrophages infected with Mycobacterium tuberculosis H37Rv strain identified by integrating bioinformatics methods. *International Journal of Molecular Medicine* 44 (4): 1243–1254. https://doi.org/10.3892/ijmm.2019.4293.
Zheng, H., L. Lu, B. Wang, S. Pu, X. Zhang, G. Zhu, W. Shi, L. Zhang, H. Wang, S. Wang, G. Zhao, and Y. Zhang. 2008. Genetic basis of virulence attenuation revealed by comparative genomic analysis of Mycobacterium tuberculosis strain H37Ra versus H37Rv. *PLoS One* 3 (6): e2375. https://doi.org/10.1371/journal.pone.0002375.

Publisher's Note